Chapter 4

Structural Transformation of Acrylic Resin Exhibits Positive and Negative Tones under Electron Beam Irradiation

Abstract

Structural transformation of polymers from linear to crosslinked structure by using electron beam irradiation has been defined as the zwitter-polymers. A resist polymer may exhibit either linear and crosslinked behavior depending on dosage of the electron beam irradiation. The property change from the structural transformation is suitable for application of positive and negative tone resists in semiconductor field. The contrast ratio and threshold dose both increase with increasing resist thickness for both the positive and negative tones, however, the positive tone exhibits better contrast than the negative tone. The intensity of the characteristic FTIR absorption bond at 1612 cm^{-1} (vinyl group) of the resist film is followed to explain the phenomena of the resist tone transformations. We have evaluated the effects of two important process conditions: the soft baking and post-exposure baking temperatures. Pattern resolution decreases upon increasing the baking temperature, except for the soft baking at the negative tone. The effect of electron doses on the pattern resolution is also discussed in detail for both tones. High electron beam exposure does not improve the resist etching resistance because of the porous nature of the resist after high dosage irradiation.

4.1. INTRODUCTION

A zwitter-polymer is a polymer with linear or crosslink properties depended on the applied doses of electron beam irradiation. The ring pattern of zwitter-polymer resist was fabricated through one shoot of electron irradiation.[1] Zwitter-polymers essentially have the properties of linear polymers, while the induced zwitter-polymers with crosslinked networks through irradiation offer the possibility of improving the strength, dimensional stability, and resistance to solvents at elevated temperatures. Furthermore, the zwitter-polymers can be used as resists with properties of both positive- and negative-tone patterns on a wafer for semiconductor applications. Thus, radiation processing offers a convenient means to form cross-linked networks in polymers, and it has attracted extensive attention in the literature.[2-5] Poly(methylmethacrylate) (PMMA) was the first to used in advanced microlithography,[6] with electron beam [7], ion beam [8], deep ultraviolet [9, 10], and x-ray radiation.[11] The increased solubility in the exposed area is caused by the degradation of PMMA by various forms of radiation. PMMA undergoes cleavage of pendent methyl ester groups and main chain scission (MCS) as a result of radiation.[12,13] Evidence for these processes includes reduced molecular weight, [6] evolution of gaseous products, [14,15] and electron-spin resonance spectroscopy. [12,16] A linear PMMA with low molecular weight is suitable for positive tone resist in semiconductor industry which can be converted into crosslink structure for zwitter-polymer.[1]

The electron-beam system has been used for many years to make the masks needed for optical lithography because of the high resolution offered by electron-beam tools. In addition, it has been noted that electron-beam (EB) irradiation is able to produce radicals along polymer chain to induce structural transformation of

polymer.[17-21] The radical-type polymerization method has been widely used for manufacturing various kinds of commercial products because of the stability of the radical species in the polymerization system compared with that in other types of polymerization systems.[22-23]

Electron-beam lithography utilizes the effect that some materials will undergo chemical changes by exposing to a beam of energetic electrons. This method has been used to fabricate high precision devices, otherwise impossible by photolithographic techniques.[24] With an electron beam writing technology, a low-density pattern can be achieved on a wafer by using a negative tone resist, while a high-density pattern usually is obtained with the aid of a positive tone resist. These strategies can be used to increase the throughput rate of a pattern by using electron beam writing techniques. Herein, we used the zwitter-polymer as the resist through electron beam writing technologies for improvement of the pattern throughput rate.

In this paper, we report in detail on the sensitivity and reaction mechanism of a zwitter-polymer after electron beam exposure. The structural transformation and glass transition temperatures (T_g) of the zwitter-polymer showing dual properties (linear and crosslinking) by Fourier transform infrared (FTIR) spectroscopy and differential-scanning calorimeter (DSC), respectively. The optimum pattern resolution for positive and negative tones of the zwitter-polymer resist for semiconductor is determined in terms of best condition of soft baking and post exposure baking. In addition, we have evaluated the lithographic behavior of positive and negative tones at different electron doses and have optimized them using an in-line SEM. The plasma resistance of the resist at different tones is also discussed.

4.2 EXPERIMENT

4.2.1 Materials and Sample Preparation

The ArF photoresist was obtained from the Sumitomo Chemical Company of Japan for electron beam exposure. The ingredients of this resist are 45–60% propylene glycol monomethyl ether acetate, 30–40% ethyl lactate, 5–20% acrylic resin, and < 1% of an acid generator. Electron beam exposure was carried out using a Leica Weprint Model-200 Stepper (Jena, Germany). The electron beam energy was 40 kV, the beam size was 20 nm, and the beam current was 40 A/cm^2. The AD-10 developer we used is an aqueous solution containing 2.38% tetramethylammonium hydroxide (TMAH; Kemitek Industrial Corp., Taiwan). Pattern dimensions were evaluated using an in-line SEM (Hitachi S-6280H, Tokyo, Japan).

The ArF resist was spun as film onto a 6-inch silicon wafer at a spin rate of 2000, 4000, or 6000 rpm (30 s duration) to give resist thicknesses of 302, 431, or 528 nm, respectively. An FTIR spectrometer (Bio-Rad, Model FTS-40, MASS, USA) was used to evaluate the variations of the resist structure during electron beam exposure. The glass transition temperature was measured with a differential-scanning calorimeter (Seiko SSC-5000) and by a wafer-curvature measurement (Tencor FLX-2320) for stress variation of thin films coated on substrate during heating procedure of imprint.

4.2.2 Sample Preparation for Plasma Etching Resistance

To test the plasma etching resistance, a silicon wafer was first primed with hexamethyldisilazane (E. Merck, Darmstadt, Germany) and then the resist was dispensed onto the wafer. The coating process was conducted by spinning at 4000 rpm for 30 s. After soft baking (110 °C, 30 s), electron beam exposure and post-exposure baking (120 °C, 30 s) were conducted. The sample was then developed with 2.38%

(w/v) tetramethylammonium hydroxide, followed by hard baking (120 °C, 30 s).

The sample prepared above was then transferred to a reactive ion etcher (Tokyo Electron Limited, Model TE-5000, Tokyo, Japan) to evaluate the plasma etching resistance of the resist. This ion etcher machine possesses a 380-kHz RF generator that is applied on both the upper and lower electrodes in a power-split mode. The respective temperatures of the upper, intermediate, and lower electrodes were 20, –13 and 40 °C. Helium gas was introduced for the wafer and the lower electrode during plasma etching to ensure better thermal conductivity. The operating conditions of etcher are listed in Table 4-1.

4.3 RESULTS AND DISCUSSION

4.3.1 The Glass Transition Temperature Measurement

The DSC method is commonly used to characterize thermal property of material. In this study, the DSC method was used to determine T_g of zwitter-polymer for resist. The heating rate was fixed at 10 °C/min. Figure 4-1 (a) shows DSC curves of the linear acrylic resin after various dosages of electron irradiations. The glass transition temperature of around 95 °C is come from the main composition of the original linear acrylic resin. Figure 4-1 (b) shows the plot of glass transition temperature of the acrylic resin with irradiated dosage by electron beam. Glass transition temperature of the acrylic resin decreases with the dosages of electron irradiations less than 30 $\mu C/cm^2$. However, the T_g increases with the dosage of electron irradiation greater than 240 $\mu C/cm^2$. This observation suggests that the linear acrylic resin was degraded by the electron exposure at low dosage irradiation, resulting in decrease of the acrylic resin molecular weight (Mw) for developing (TMAH) of the semiconductor process. This behavior performs the function of a positive tone resist. At the same time, the

vinyl groups were created in these low molecular weight acrylic resin molecules after low dosage of electron irradiation [25]. These low Mw acrylic resin molecules containing vinyl groups are able to repolymerize by electron beam irradiation under higher dosage and thus result in crosslinking and increase of molecular weight. Therefore, the modified acrylic resin (crosslinked) can no longer be developed by TMAH and exhibit behavior of negative tone resist. The approximate glass transition temperature of acrylic resin modified by electron irradiation is closed to 109 °C, which is substantially higher than T_g of the original linear acrylic resin. The repolymerization results in crosslinking for the acrylic resin after electron exposure and thus higher T_g. The glass transition temperature of acrylic resin modified by electron irradiation is not obviously defined from DSC measurement because of the crosslinked nature.

4.3.2 Mechanism of the Chemical Reaction of the Zwitter-polymer upon Electron Eeam Irradiation

The FTIR absorption spectra of the acrylic resin film were measured for qualitative and quantitative analysis of the degradation process caused by E-beam irradiation. The major gaseous products formed from the acrylic resin under E-beam irradiation are methyl formate, methane (or $\cdot CH_3$), methanol, CO, and CO_2 along with many other products.[26, 27] The following E-beam irradiation transforms the linear acrylic resin into crosslinked acrylic resin resist, shifting from a positive tone into a negative tone. Figure 4-2 provides FTIR spectra of zwitter-polymer film at both of linear and crosslink tones. The absorption peak at 1612 cm^{-1} represents the characteristic vibration of the C=C bond.[25] For the linear acrylic resin from low dosage irradiation (Figure 4-2 a), this characteristic absorption peak (1612 cm^{-1})

increases upon increasing the applied dose in the range from 0 to 30 $\mu C/cm^2$, an indication of the acrylic resin degradation resulting in more radicals and C=C bonds. High dosage irradiation induces the acrylic resin crosslinking (Figure 4-2b), thus the 1612 cm^{-1} absorption peak decreases with the increase of the applied dose in the range from 240 to 320 $\mu C/cm^2$. The absorption peak at 1612 cm^{-1} irradiated with 150 $\mu C/cm^2$ of dosage is used to be 1 for normalizing the intensity of the absorption peak as shown in Figure 4-2 (c). The normalized intensity of absorption peak at 1612 cm^{-1} increases rapidly as the dosage is below 30 $\mu C/cm^2$, indicating the extreme sensitivity of the linear acrylic resin. The normalized intensity maintains a constant value as the dosage is from 30 to 240 $\mu C/cm^2$. Above 240 $\mu C/cm^2$, the irradiation induces crosslinking polymerization of the vinyl group, resulting in the decrease of the normalized intensity of the vinyl group.

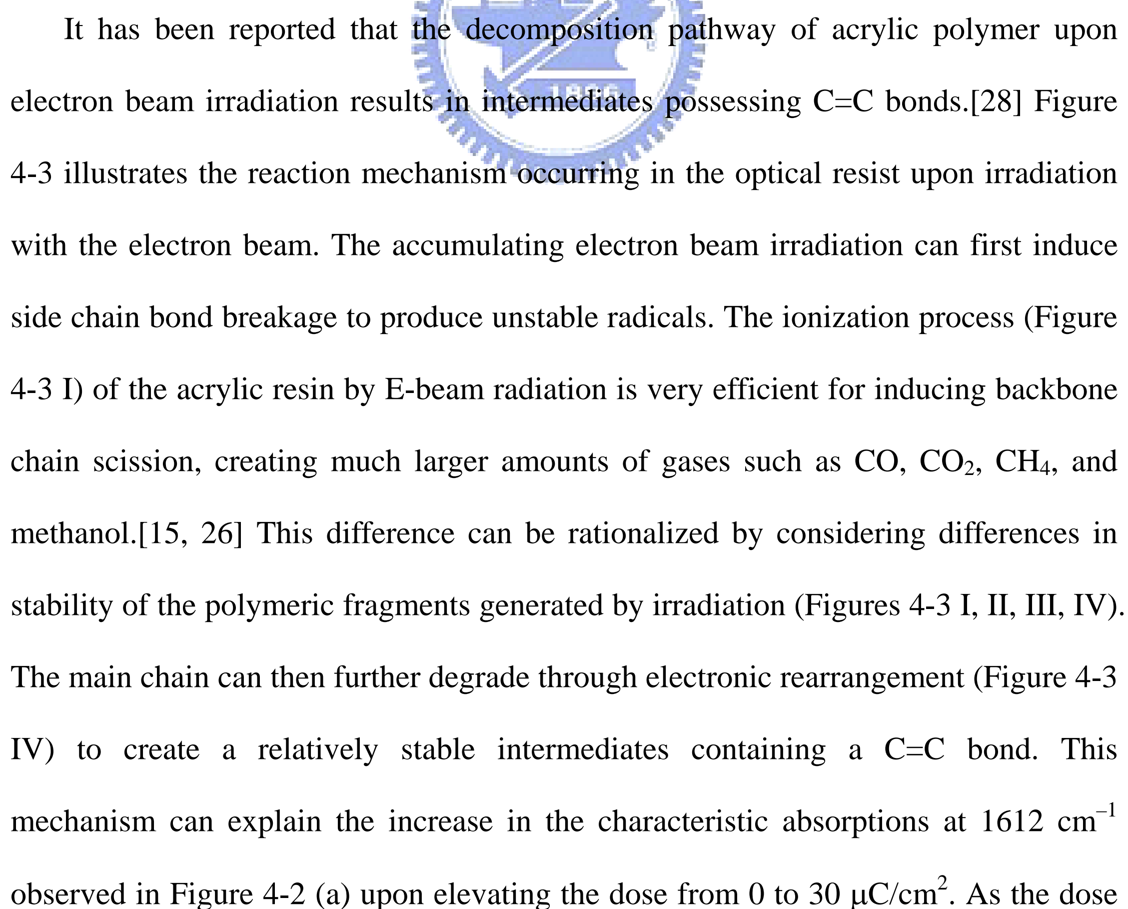

It has been reported that the decomposition pathway of acrylic polymer upon electron beam irradiation results in intermediates possessing C=C bonds.[28] Figure 4-3 illustrates the reaction mechanism occurring in the optical resist upon irradiation with the electron beam. The accumulating electron beam irradiation can first induce side chain bond breakage to produce unstable radicals. The ionization process (Figure 4-3 I) of the acrylic resin by E-beam radiation is very efficient for inducing backbone chain scission, creating much larger amounts of gases such as CO, CO_2, CH_4, and methanol.[15, 26] This difference can be rationalized by considering differences in stability of the polymeric fragments generated by irradiation (Figures 4-3 I, II, III, IV). The main chain can then further degrade through electronic rearrangement (Figure 4-3 IV) to create a relatively stable intermediates containing a C=C bond. This mechanism can explain the increase in the characteristic absorptions at 1612 cm^{-1} observed in Figure 4-2 (a) upon elevating the dose from 0 to 30 $\mu C/cm^2$. As the dose

approached to 240 μC/cm^2, the C=C bond-containing intermediate, which is susceptible to the electron beam, can undergo crosslinking polymerization (Figure 4-3 V). Therefore, the intermediate species containing C=C bonds disappear as shown in Figure 4-2 b. The macromolecule formed by crosslinking can no longer to be dissolved in the developer (TMAH), which explains its negative tone behavior (Figure 4-2 b).

4.3.3 Sensitivity Curves

In general, linear polymers are used as positive tone resists for semiconductor, such as PMMA, while the crosslinked polymers are used as negative tone patterns on wafer. The zwitter-polymer is able to play a role of both positive and negative tone resists simultaneously for electron beam lithography. On the other hand, the trenches and lines patterns can fabricate on the same layer by one shoot of electron irradiation. Figure 4-4 presents the sensitivity curves of the zwitter-polymer resist. This acrylic resin resist exhibits a positive tone as the dosage is below 30 μC/cm^2 and shifts into a negative tone for dosages > 300 μC/cm^2.[1] The contrast ratios and threshold doses obtained from the sensitivity curves are listed in Table 4-2. As indicated in the Table 4-2 where the contrast ratio and threshold dose both increase with increasing resist thickness for both positive and negative tones. These observations suggest that the resist film of greater thicknesses requires higher doses to exhibit desirable lithographic behavior and the contrast of the resist does not deteriorate. Figure 4-4 clearly shows that the acrylic resin resist has excellent response under the electron beam irradiation according to these sharp sensitivity curves. Table 4-2 shows that the contrast ratios for the positive tone resist are about trice as those of the negative tone resist.

4.3.4 Effect of Baking Zwitter-polymer Resists for Pattern Resolution

(1) Positive tone (linear acrylic resin)

In electron beam lithography, a positive-tone resist is suitable for patterning trenches and holes. Figure 4-5 presents the effect of soft baking and post exposure baking temperatures on trench resolution for a zwitter-polymer resist displaying a positive tone. The trench width increases upon increasing the soft baking temperature from 100 to 130 °C with the same post-exposure baking conditions. As mentioned in the experimental section, the optical resist contains an acid generator and a solvent. The tendency to increase the trench width with increasing soft baking temperature is probably due to the effect of acid diffusion. The amount of residual solvent in the resist decreases when the soft baking temperature is increased, and results in the sensitivity increase of the acid generator. Higher soft baking temperature with lower solvent content is a more suitable condition for diffusion of the acid generator during the post-exposure baking step. Hence, the trench width increases when the soft baking temperature is increased. Furthermore, the trench width, with respect to the soft baking temperature, reaches a plateau because most of the solvent in the resist film is already vaporized above 120 °C. The trench width also increases with the increase of the post-exposure baking temperature from 100 to 130 °C when the same soft baking conditions are applied. This result can be interpreted as the higher post-exposure temperature inducing a greater diffusion distance of the acid generator.

(2) Negative Tone (crosslinked acrylic resin)

In electron beam lithography, a negative-tone resist is suitable for line patterning. The resist with negative tone is achieved as the electron beam dosage is greater than

240 μC/cm^2, indicating that the acrylic resin with vinyl groups repolymerized to form the crosslinked acrylic resin as shown in pathway V of Figure 4-3. Figure 4-6 illustrates the effect of the soft baking and post exposure baking conditions on line width of the zwitter-polymer resist having negative tone. The line width decreases upon increasing the temperature of the soft baking from 100 to 130 °C under the same post-exposure baking conditions. The residual solvent content in the resist decreases by raising the soft baking temperature. The resist at a lower soft baking temperature contains more solvent, and, hence, possesses greater subsequent electron beam absorbance ability than that at a higher soft baking temperature. As a result, a lower soft baking temperature causes higher extent of species of repolymerization (Figure 4-3 V) and leads to a wider line.

In contrast, the line width increases upon increase of the post-exposure baking temperature from 100 to 130 °C under the same soft baking conditions. The effect of post-exposure baking temperature of the negative tone (Figure 6) shows similar trend as the positive tone (Figure 4-5). Higher post-exposure baking temperature results in higher extent of crosslinkage and thus greater line width.

4.3.5 Resolution of Positive and Negative Behaviors

(1) Positive Tone (linear acrylic resin)

Figure 4-7 (a) illustrates the relationship between the designed trench width and the measured trench width for various doses. Interestingly, the measured trench width increases linearly with the designed trench width for the doses of interest as shown in Figure 4-7 (b). This observation suggests that both suitability and controllability are obtainable by using the positive-tone resist. Furthermore, as shown in the Figure 4-7 (b), the measured trench width increases with the applied dose in all dimensions of the

designed trenches. The measured trench width is equal to that of the designed trench at a dose of 8.5 $\mu C/cm^2$. Figure 4-7 (c) displays the minimal resolution of dense trenches of 92 nm obtained at a dose of 7 $\mu C/cm^2$. These trenches are all very straight and the line-edge roughness (LER, in 3σ) is ca. 2.1. Figure 4-7 (d) presents an in-line SEM image of a contact hole, the minimal resolution is ca. 115 nm.

(2) Negative Tone (crosslinked acrylic resin)

Figure 4-8 (a) illustrates the relationship between the designed and measured line widths at various electron beam doses. The measured line width also increases linearly with the designed line width for the doses of interest. This observation also suggests the suitability and controllability of the negative-tone resist. Again, the measured line width increases with increasing applied dosage in all dimensions of the designed line as displayed in Figure 4-8 (b). The measured line width is equal to the designed trench width at a dose of 880 $\mu C/cm^2$. The minimal resolution of the dense line is 104 nm, as indicated in Figure 4-8 (c), which is achieved by using a dose of 900 $\mu C/cm^2$. These lines are also very straight and the line edge roughness (LER, in 3σ) is ca. 2.2.

4.3.6 Etching Behavior of Zwitter-polymer Resist

A reactive ion etcher has been used to evaluate the etching resistance for both positive and negative tones of the zwitter-polymer resist on a silicon dioxide layer. The feeding gas was a mixture of Ar, CHF_3, and CF_4. The chemical species present in the plasma can be expressed as follows:[29, 30]

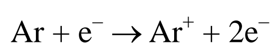

$$Ar + e^- \rightarrow Ar^+ + 2e^-$$

$$CF_4 + e^- \rightarrow CF_3^+ + F^- + e^-$$

$$CF_3^+ + F^- \rightarrow CF_4$$

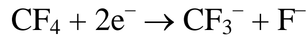

$$CF_4 + 2e^- \rightarrow CF_3^- + F^-$$

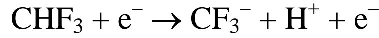

$$CHF_3 + e^- \rightarrow CF_3^- + H^+ + e^-$$

$$CF_3^+ + CF_3^- \rightarrow C_2F_6$$

$$SiO_2 + CF_3^+ + F^- \rightarrow SiF_4 + CO_2$$

The CF_3^+ and F^- species generated in the plasma can react with the silicon dioxide film to form the volatile species of SiF_4 and CO_2 and, therefore, the silicon dioxide film becomes etched. In addition, these radicals, atoms, and ions generated can also react with the zwitter-polymer resist to form various volatile products such as CO, CO_2, H_2O, OH, and COF_2. Therefore, the plasma resistance of the resist is very critical to ensure etch reliability. Figure 4-9 (a) displays that the etching rate decreases with increasing CHF_3 content in the CHF_3/CF_4 mixture for both zwitter-polymer resist and silicon dioxide film. This observation can be explained by the role of CHF_3 plays in the plasma. The species generated from CHF_3 playing in the plasma are the formation of H^+ and CF_3^-. The CF_3^- can retard the activity of the CF_3^+ in the plasma and thus results in etching rate decrease. Interestingly, the etching resistance of the negative tone of the zwitter-polymer resist is a slightly lower than that of the positive tone at any gas composition. This finding suggests that the resist of negative tone formed by a very high electron beam dose (> 240 $\mu C/cm^2$) may cause porous property of crosslinked structure, resulting in lower plasma resistant than that of positive-tone resist. It has been reported [31, 32] that electron beam exposure can stabilize a resist film and enhance its etch resistance. However, it is valid only for those with relatively low doses of electron beam irradiation. It can be concluded the electron beam exposure facilitates etch resistance of the resist in the low-dose region, but higher

dose exposure (> 240 μC/cm^2) results in the inverse effect.

Figure 4-9 (b) illustrates the etch selectivity (etch rate of silicon dioxide relative to that of the zwitter-polymer resist) for various compositions of etching gases. The etch selectivity increases from 7.9 to 10.7 for the positive tone upon increasing the CHF_3 content, while it increases from 5.9 to 8.5 for the negative tone. In general, the etch selectivity of the positive tone is better than that of the negative tone because of the dose effect. The better etch resistance of the zwitter-polymer resist (selectivity > 5) emphasizes its potential for use in patterning silicon dioxide layers.

4.4 CONCLUSIONS

The structure of a resist polymer with linear, crosslinked or a mixture of both can be controlled through electron beam irradiation. Structural transformation of the acrylic resin from linear to crosslinking is suitable for applications of positive tone and negative tone resists. The acrylic resin, a zwitter-polymer resist, exhibits a positive tone when the dosage is in the range 3–300 μC/cm^2, and a negative tone for dosages > 300 μC/cm^2. The contrast ratio for the positive tone is about trice as the negative tones, the lower contrast ratio of the latter is caused by higher threshold dose. The reverse trend of the intensity of the characteristic absorption band at 1626 cm^{-1} of the resist is responsible for the resultant positive- and negative-tone behaviors. The chemical chain scission occurs at low electron dose and crosslinking occurs at high dose are responsible for the positive tone and negative tone, respectively. In the positive tone, the solvent content at various soft baking temperatures affects the pattern resolution, while the diffusion distance of the acid generator at various post-exposure baking temperatures affects the pattern resolution. In the negative tone, various soft baking temperatures affect the pattern resolution, while degree of

crosslinkage at various post-exposure baking temperatures affects the pattern resolution. The measured trench width is equal to that of the designed trench at a dose of 8.5 μC/cm^2 for positive tone, and at a dose of 880 μC/cm^2 for negative tone. The electron beam exposure facilitates etch resistance of the resist in the low-dose region, results in the inverse effect at higher dosage irradiation.

REFERENCES

1 J. K. Chen; F. H. Ko; H. L. Chen; F. C. Chang. *Jpn. J. Appl. Phys.*, **42**, 3838 (2003).

2. E. Katoh; H. Sugishwa; A. Oshima; Y. Tabata; T. Seguchi; T. Yamazaki. *Radiat. Phys. Chem.*, **54**, 165 (1999).

3. B. Fuchs; U. Scheler. *Macromolecules*, **33**, 120 (2000).

4. B. Fuchs; U. Lappan; K. Lunkwitz; U. Scheler. *Macromolecules*, **35**, 9079 (2002).

5. T. R. Dargaville; G. A. George; D. J. T. Hill; U. Scheler; A. K. Whittaker. *Macromolecules*, **36**, 7138 (2003).

6.C. G. Willson. *Introduction to Microlithography*, edited by L. F. Thompson, C. G. Willson, and M. J. Bowden, 123.

7. W. M. Moreau; *Submicron Lithography* (SPIE),2.

8. R. G. Brault; L. J. Miller. *Polym. Eng. Sci*. **20(16)**, 1064 (1980).

9. B. J. Lin. *J. Vac. Sci. Technol B*. **12**, 1317 (1975).

10. Y. Minura; T. Ohkubo; T. Takeuchi; K. Sekikawa. *Jpn. J. Appl. Phys*. **17(6)**, 1317 (1975).

11. H. Sotobayashi; F. Asmussen; K Thimru; W. Schnatel; H. Betz; D. Einfeld. *Polym. Bull*.**7**.95 (1980).

12. A. Gupta; R. Liang; F. D. Tsay; J. Moscanin. *Micromolecules*. 13, 1696 (1980).

13. A. Tadd. *J. Polym. Sci*. **42**, 223 (1960).

14. R. B. Fox; L. G. Isaacs; S. Stokes. *J. Polym. Sci. Part A*. **1**, 1079 (1963).

15. C. David; D. Fuld; G. Genuskens. *Macromolecular Chem*. **139**, 269 (1970).

16. C. R. Chen; R. I. Knight; L. Pollock. *J. Polym. Sci. Part A*. **25**, 127 (1987).

17. K. Miyazaki; K. Hisada; T. Hori; Y. Kondo; E. Saji; T. Kimura. *Sen-i Gakkaishi*, **56**, 126 (2000).

18. S. Tsuneda; K. Saito; T. Sugo; K. Makuuchi. *Radiat Phys Chem*, **46**, 239 (1995).

19. S. Tsuneda; K. Saito; H. Mitsuhara; T. Sugo. *J Electrochem Soc*, **142**, 3659 (1995).

20. K. Uezu; K. Saito; S. Furusaki; T. Sugo; I. Ishigaki. *Radiat Phys Chem*, **40**, 31 (1992).

21. J. E. Wilson. *J Macromol Sci Chem*, **8**, 307 (1974).

22. General reviews on living radical polymerization: (a) C. Hawker. *J. Acc. Chem. Res.*, **30**, 373 (1997). (b) J. Xia; K. Matyjaszewski. *Chem. Rev.*, **101**, 2921 (2001).

23. (a) T. E. Patten; J. Xia; T. Abernathyl; K. Matyjaszewski. *Science*, **272**, 866 (1996). (b) S. Liu; J. V. M. Weaver; Y. Tang; N. C. Billingham; S. P. Armes; K. Tribe. *Macromolecules*, **35**, 6121 (2002). (c) J. F. Hester; P. Banerjee; Y. Y. Won; A. Akthankul; M. H. Acar; A. M. Mayes. *Macromolecules*, **35**, 7652 (2002). (d) S. Lu; Q. L. Fan; S. Y. Liu; S. J. Chua; W. Huang. *Macromolecules*, **35**, 9875 (2002).

24. W. H. Wong; J. Zhou; E. Y. B. Pun. *Appl. Phys. Lett.*, **78**, 2110 (2001).

25. J. O. Choi, J. A. Moore, J. C. Corelli, J. P. Silverman; H. Bakhru. *J. Vac. Sci. Technol., B,* **6**, 2286 (1988).

26. H. Hiraoka. *IBM J. Res. Dev*. **21**, 121 (1977)

27. A. R. Shultz. *J. Polym. Sci*. **35**, 369 (1959).

28. K. Biemann; Spectral Data for Structure Determination of Organic Compounds

(Springer-Verlag, Berlin, 1983).

29. C. Y. Chang; S. M. Sze. ULSI Technology (McGraw-Hill, New York, 1996).

30. S. Wolf; R. Tauber; Silicon Processing for the VLSI Era, Vol. 1 (Lattice Press, California, 1986), Chapter 16.

31. P. Martens, S. Yamamoto, K. Edamatsu, Y. Uetani, L. Pain, R. Palla, M. Ross; W. Livesay. Proc. SPIE, **4345**, 138 (2001).

32. T. Sarubbi; M. Ross; M. Neisser; T. Kocab; B. Beauchemin; W. Livesay; S. Wong. Proc. SPIE, **4345**, 211 (2001).

Table 4-1 Operating conditions for the reactive ion etcher

	Step 1	Step 2
Pressure/Torr	0.2	0.2
RF power/W	0	500
Gas flow rate/$cm^3 min^{-1}$		
Ar	400	400
CHF_3	10–30	10–30
CF_4	30–10	30–10

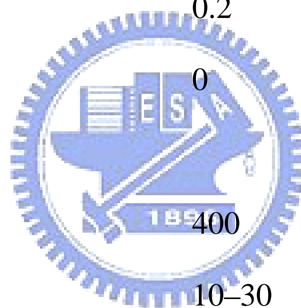

Table 4-2. Contrast ratios[a] (γ) and threshold doses[a] (E_{th}) for the zwitter-polymer resist at various thicknesses.[b]

Resist Thickness (nm)	Positive tone		Negative tone	
	γ	E_{th} ($\mu C/cm^2$)	γ	E_{th} ($\mu C/cm^2$)
302	8.49	3.6	4.15	220
427	9.24	3.9	4.82	260
523	9.49	5	5.82	320

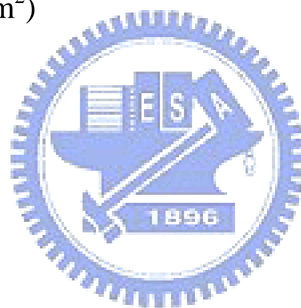

[a] Definitions of contrast ratio and threshold dose are provided in Chapter1.

[b] Soft baking was performed at 110 °C for 90 s and post-exposure baking at 125 °C for 60 s.

(a)

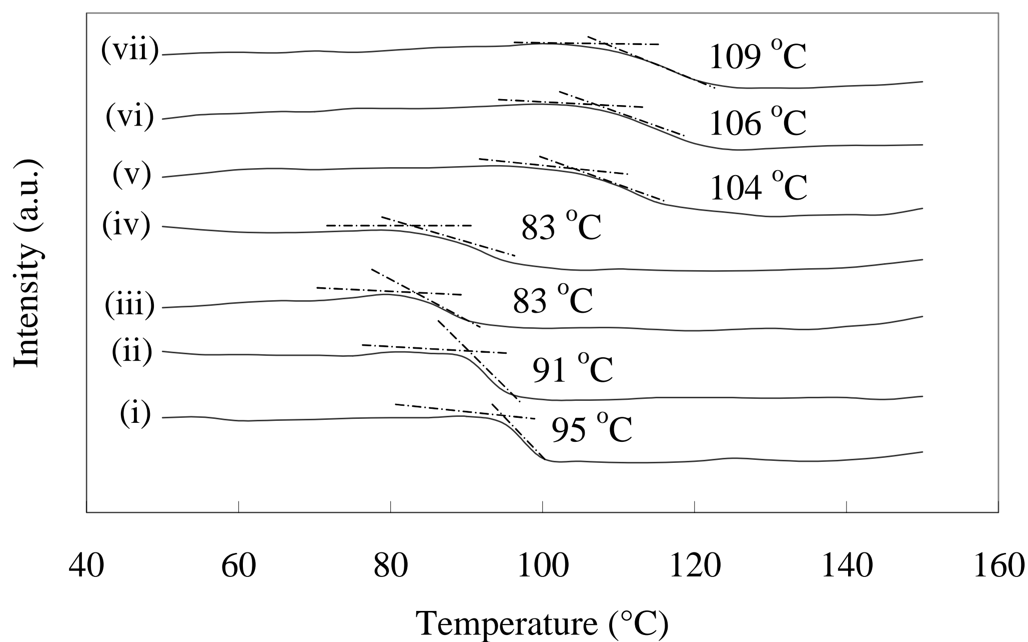

(b)

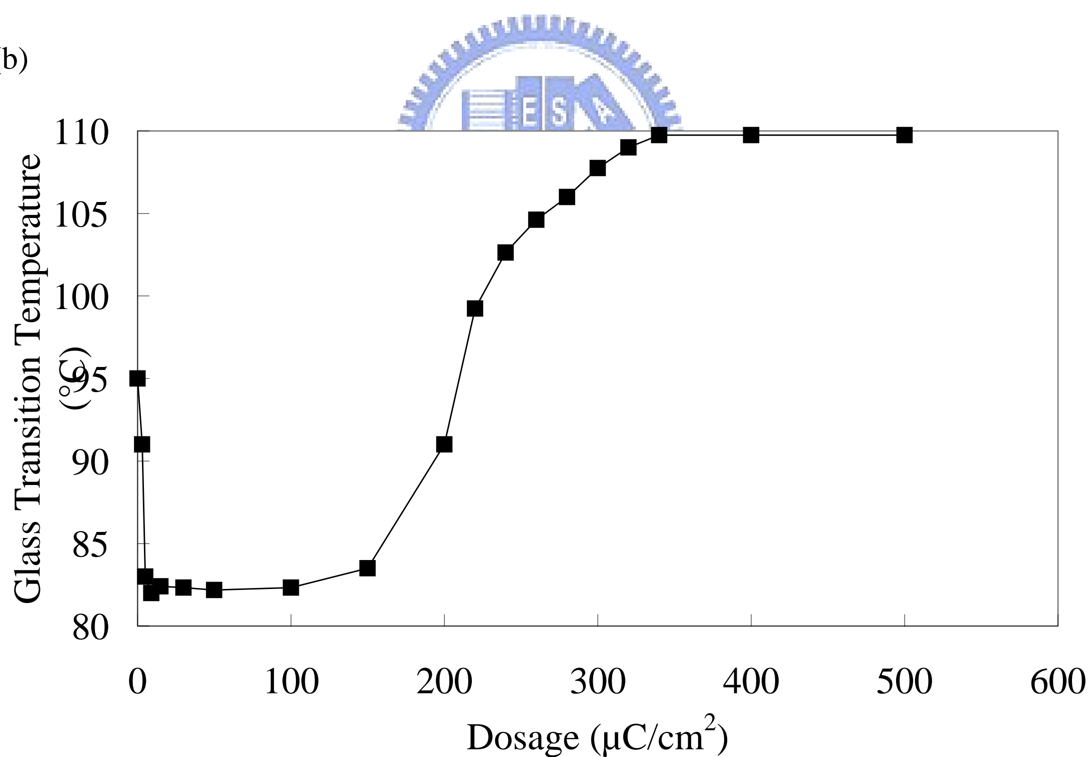

Figure 4-1. (a) DSC curves of the zwitter-polymer under electron beam irradiation with (i) 0, (ii)3, (iii)5, (iv) 7, (v) 240, (vi)280, and (vii)320 $\mu C/cm^2$ of dosage. (b) The plot of glass transition temperature with irradiated dosage by electron beam.

(a)

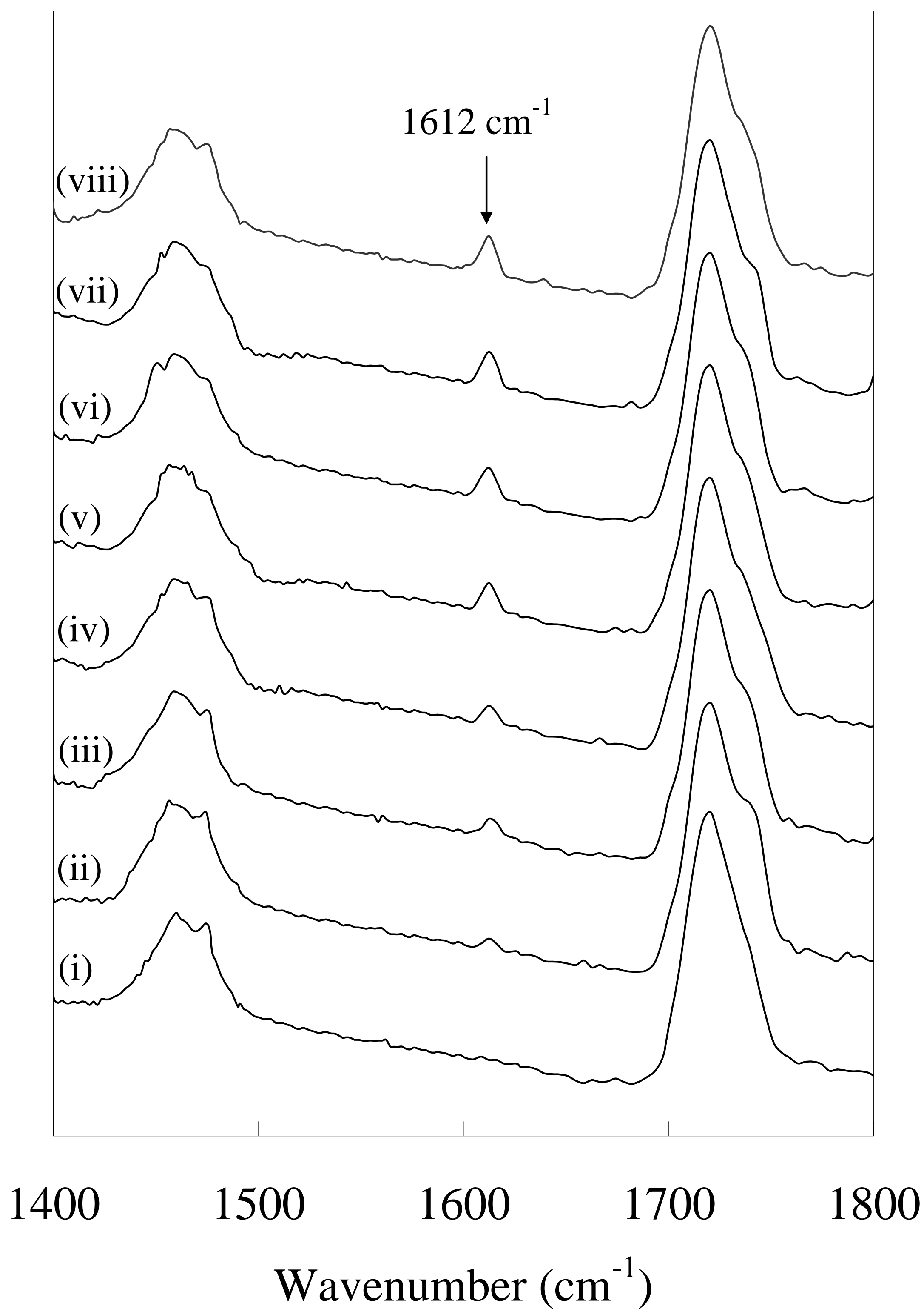

Figure 4-2. Various FTIR spectra of zwitter-polymer resist films at different electron beam doses: (a) positive tone after electron beam doses of 0, 1, 3, 5, 7, 9, 15, and 30 μC/cm^2.

(b)

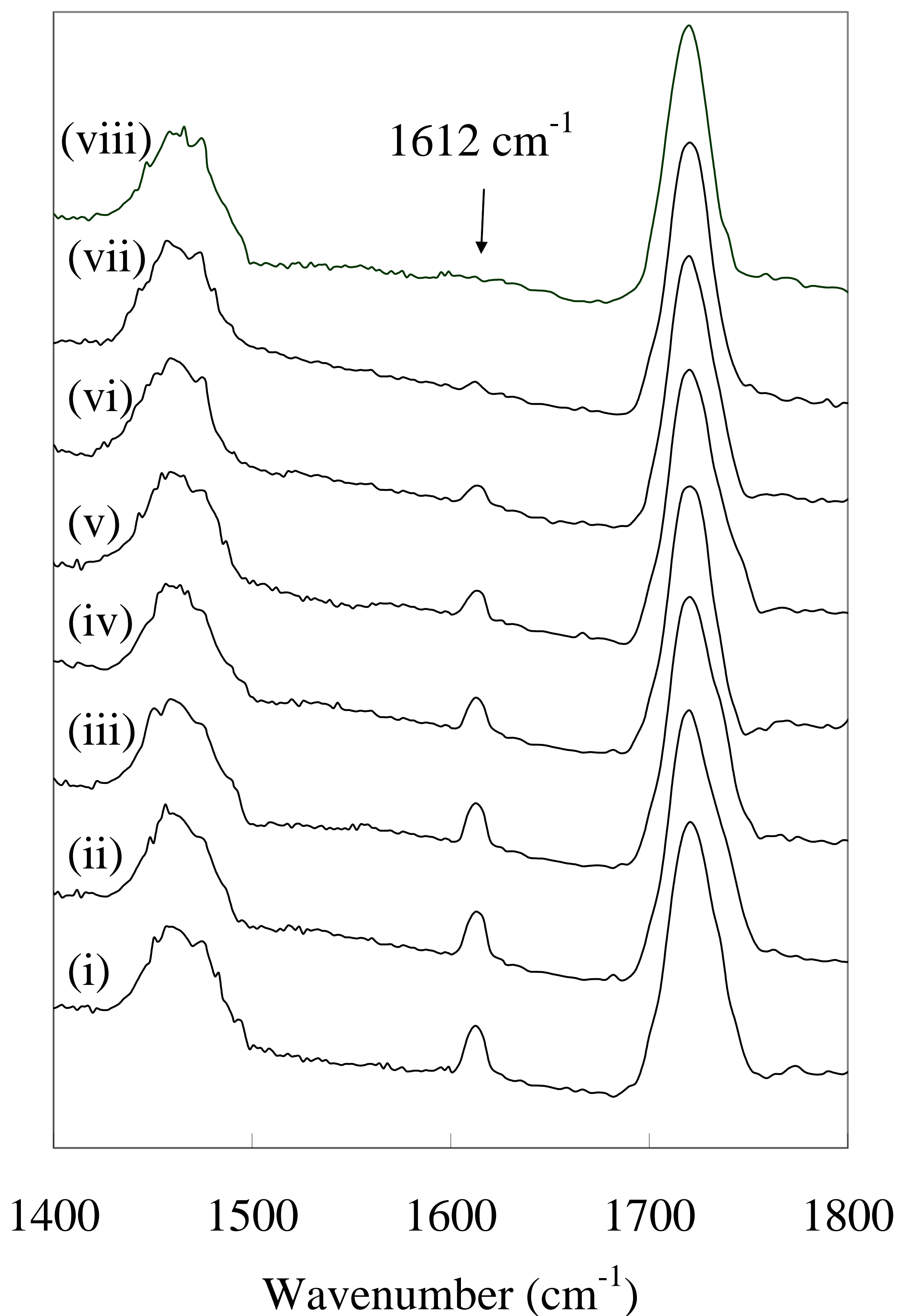

Figure 4-2. (b) Negative tone after electron beam doses of (i) 240, (ii) 250, (iii) 260, (iv) 270, (v) 280, (vi) 290, (vii) 300, and (viii) 320 μC/cm^2.

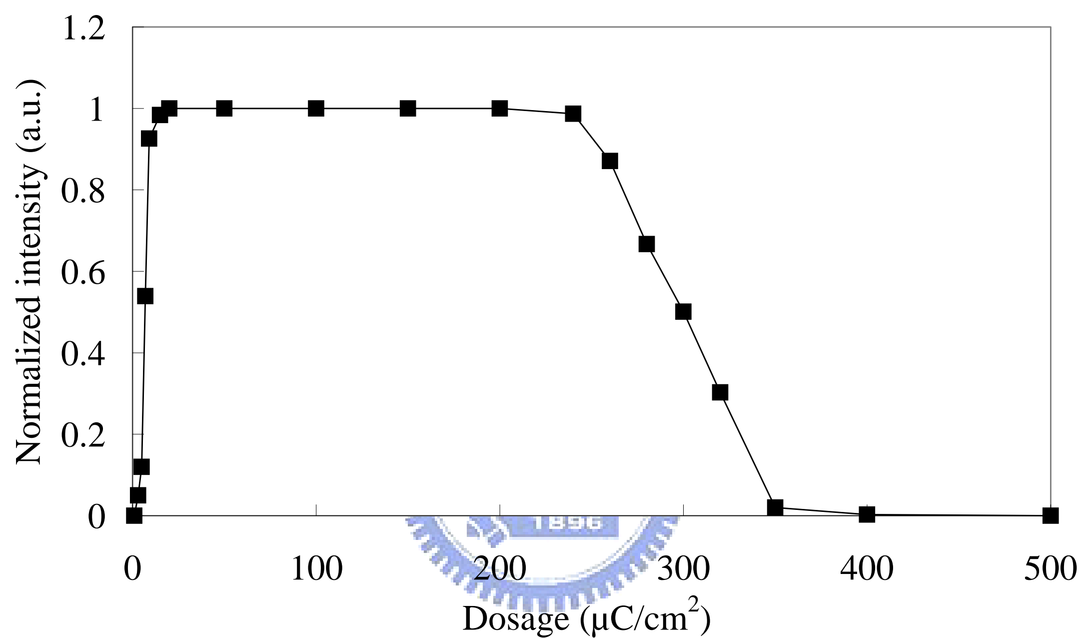

Figure 4-2. (c) The normalized intensity of various FTIR absorption peak at 1612 cm^{-1} as a function of electron beam irradiation dosage.

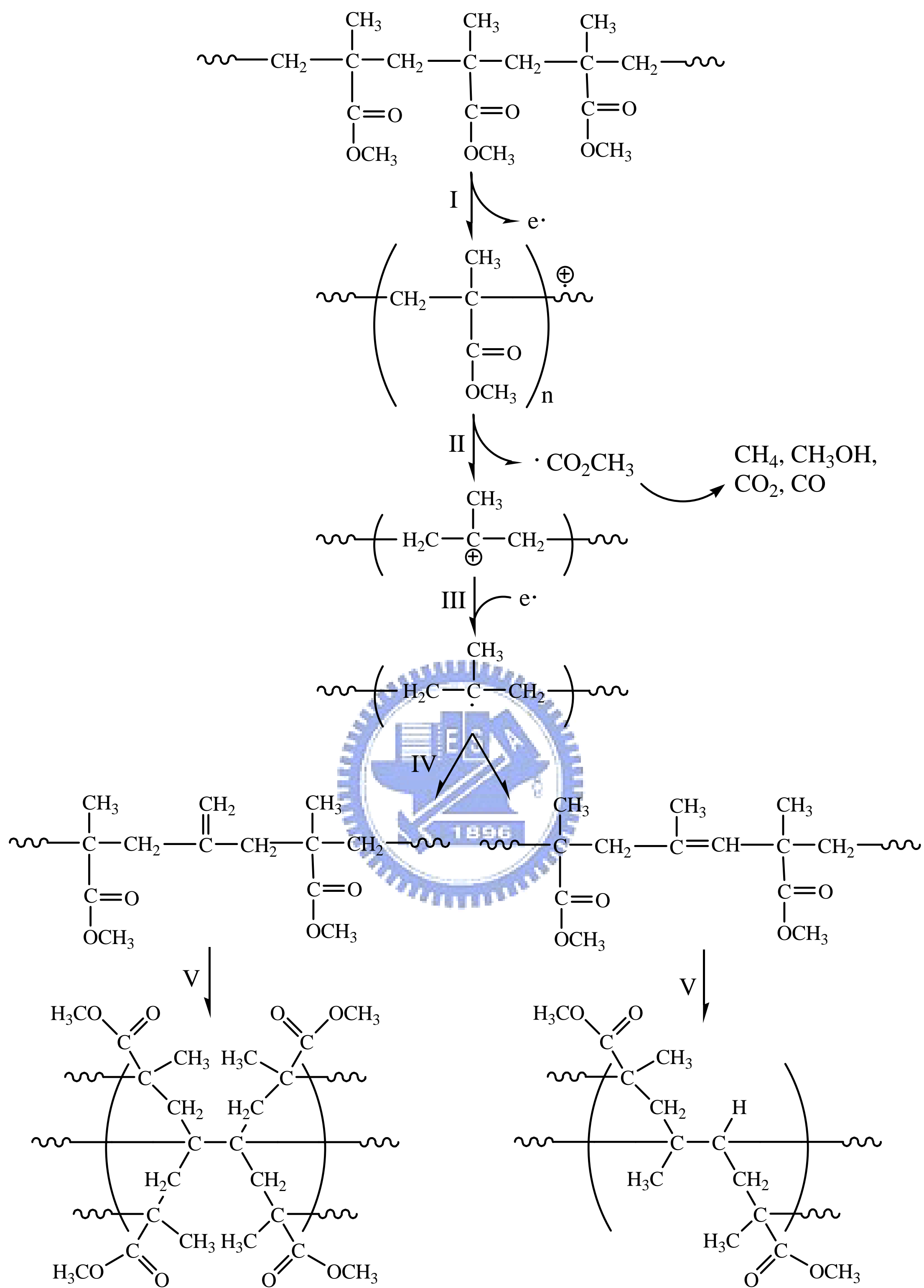

Figure 4-3. Reaction mechanisms of the reactions occurring in the zwitter-polymer resist upon exposure to an electron beam.

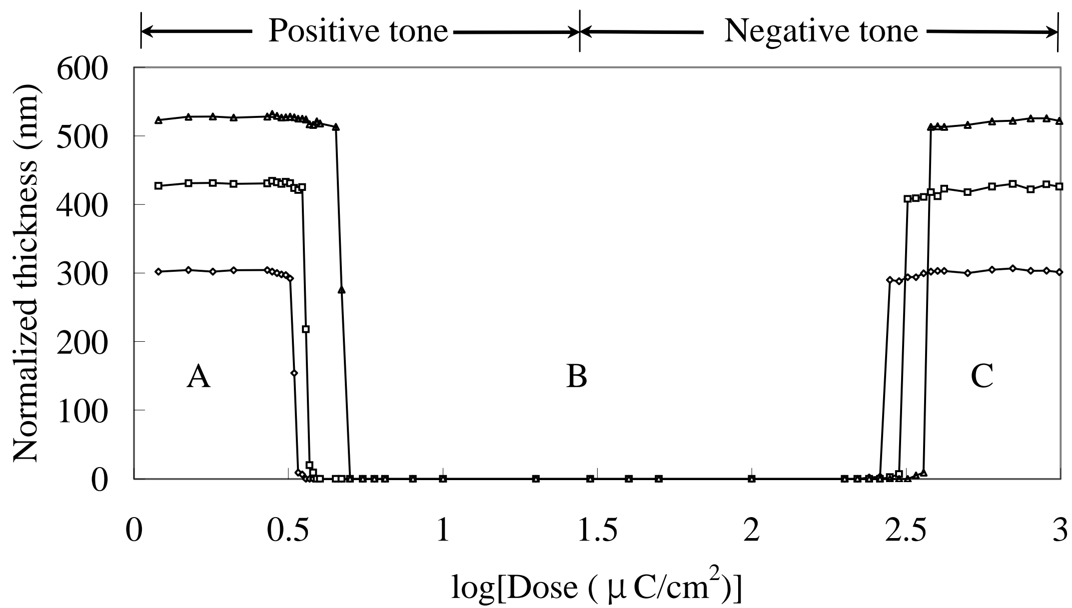

Figure 4-4. Sensitivity curves for the zwitter-polymer resist at an electron beam exposure of 40 keV for various film thicknesses.

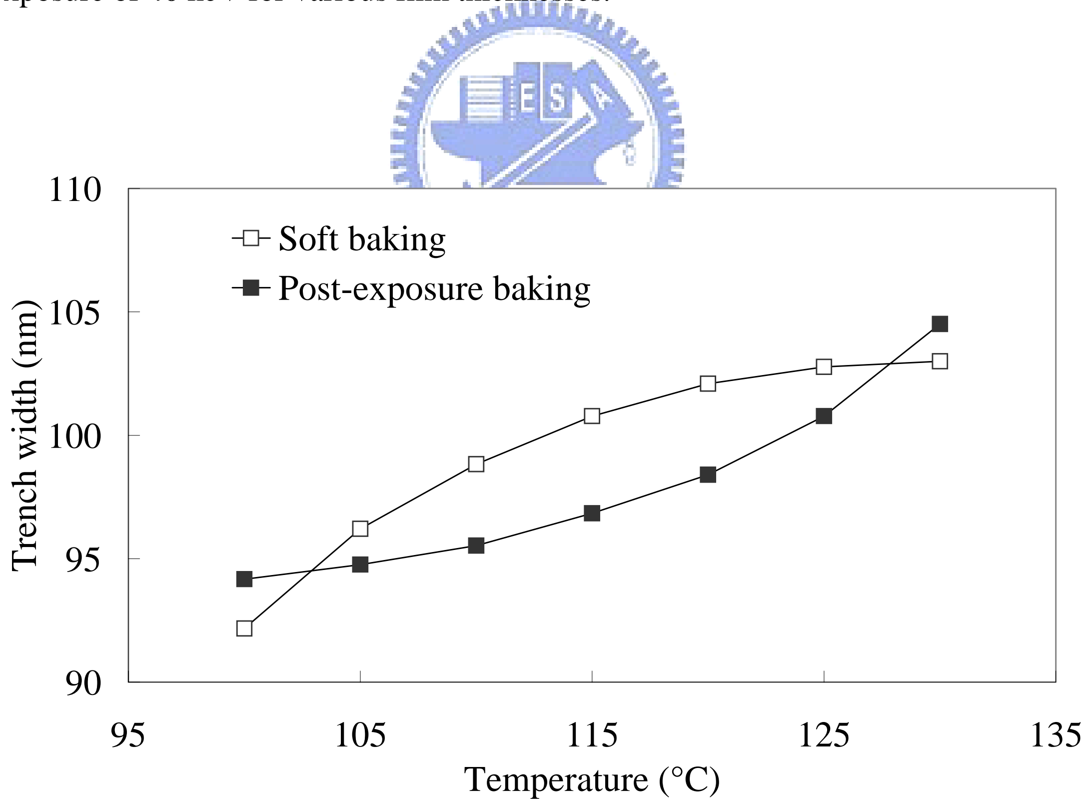

Figure 4-5. The effects of soft baking and post-exposure baking (PEB) on the trench width of the positive-tone zwitter-polymer resist.

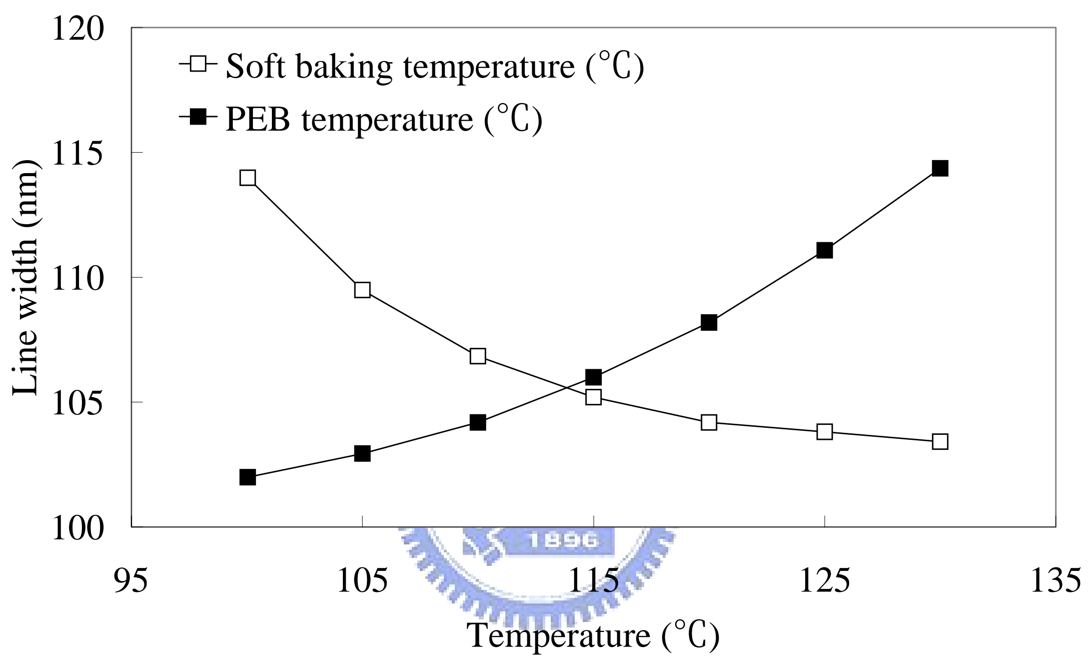

Figure 4-6. The effect of soft baking and post-exposure baking (PEB) on the line width of the negative-tone zwitter-polymer resist.

(a)

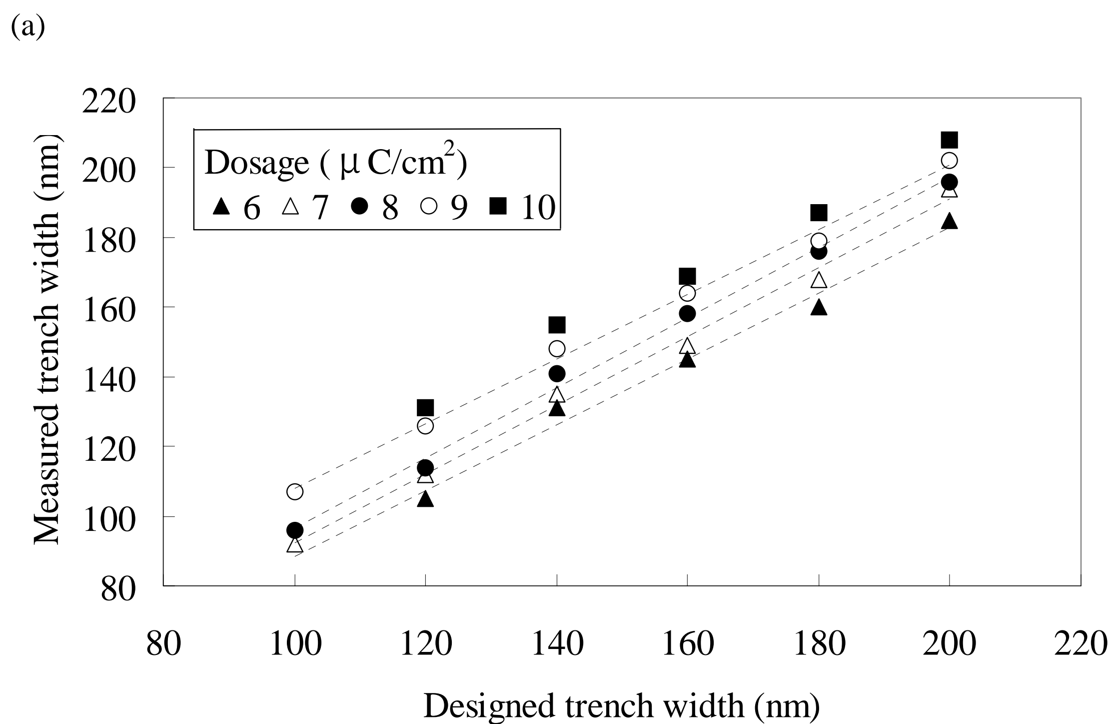

(b)

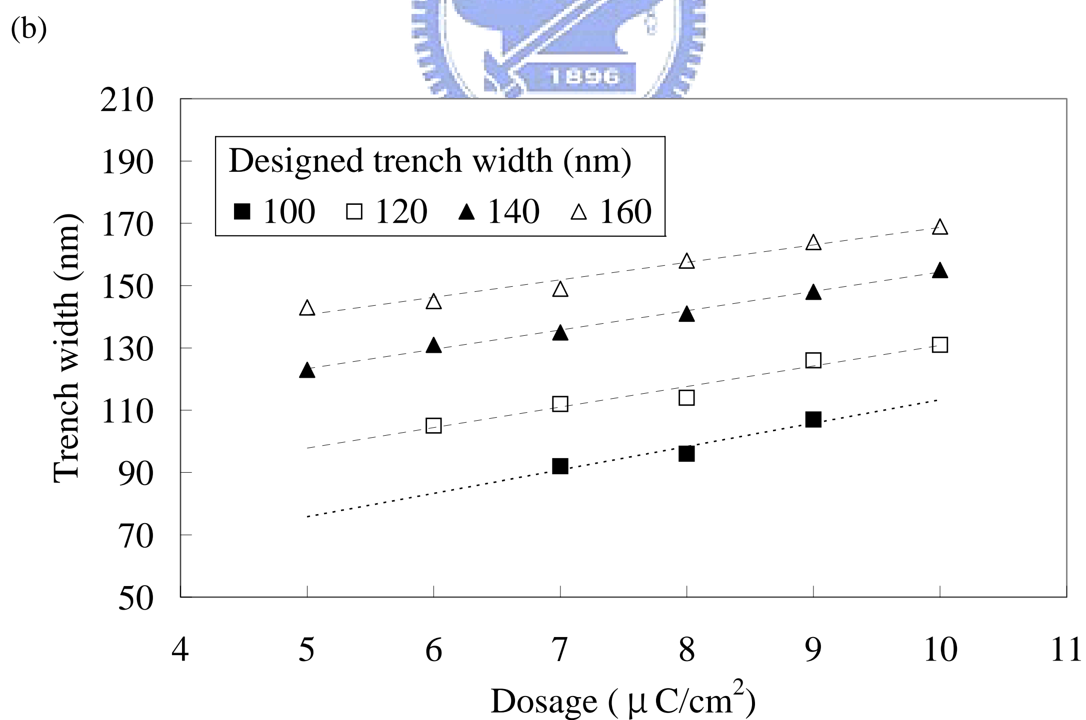

Figure 4-7. The effect of dosage on pattern resolution for the positive-tone zwitter-polymer resist: (a) plot of designed trench width vs. obtained trench width; (b) plot of dosage vs. trench width.

(c)

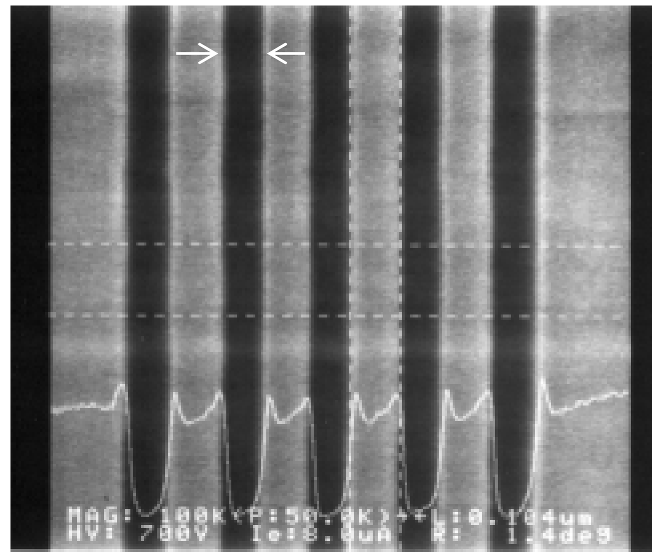

(d)

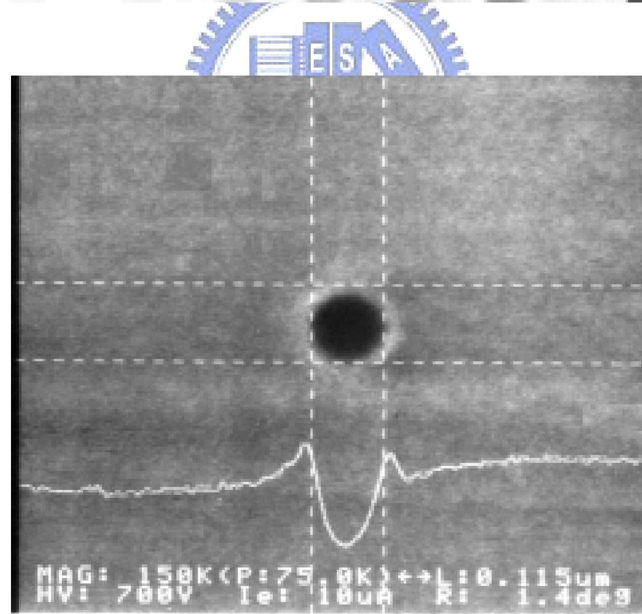

Figure 4-7. The effect of dosage on pattern resolution for the positive-tone zwitter-polymer resist: (c) image of dense trenches having 92-nm width; (d) image of a hole of 115-nm diameter.

(a)

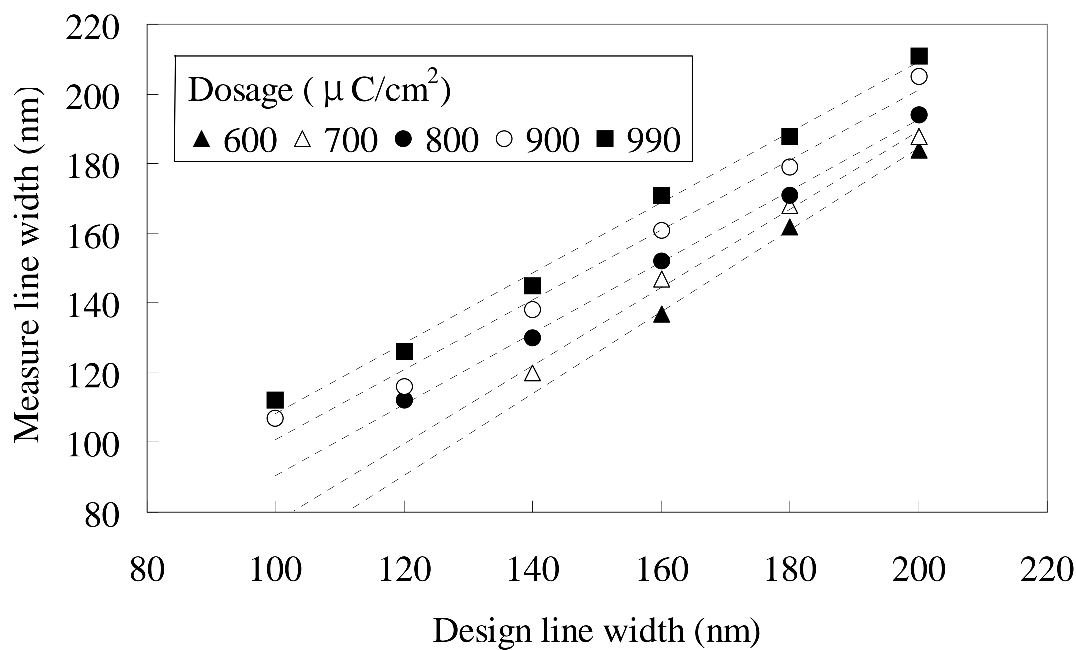

(b)

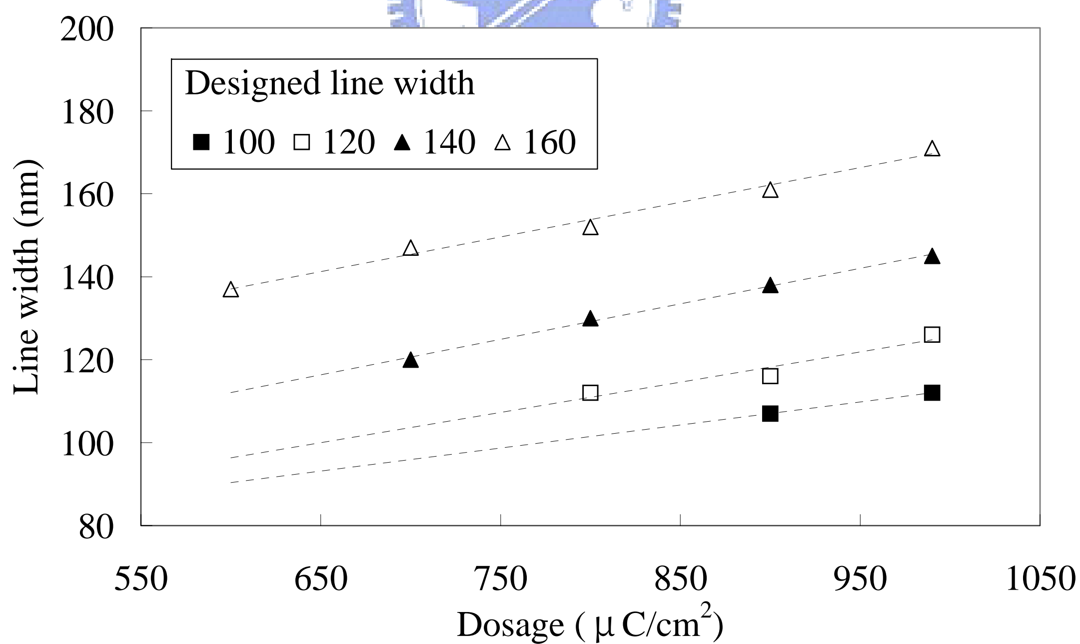

Figure 4-8. The effect of dosage on pattern resolution for the negative-tone zwitter-polymer resist: (a) plot of designed line width vs. obtained line width; (b) plot of dosage vs. line width.

(c)

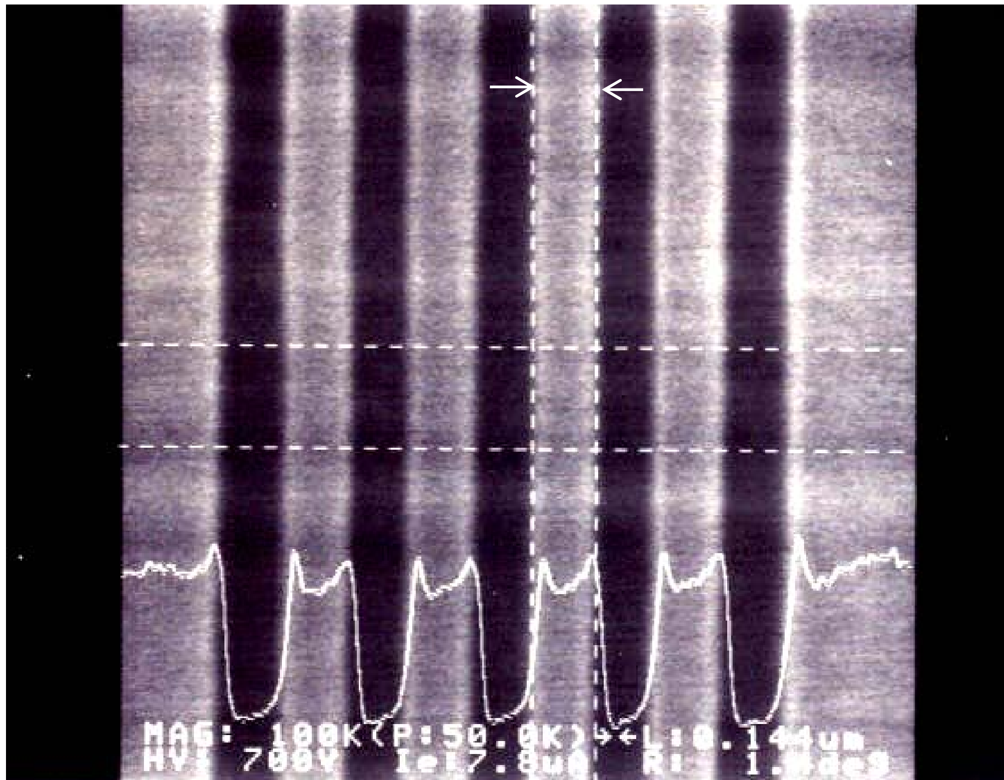

Figure 4-8. The effect of dosage on pattern resolution for the negative-tone zwitter-polymer resist: (c) image of 104-nm-wide dense lines.

(a)

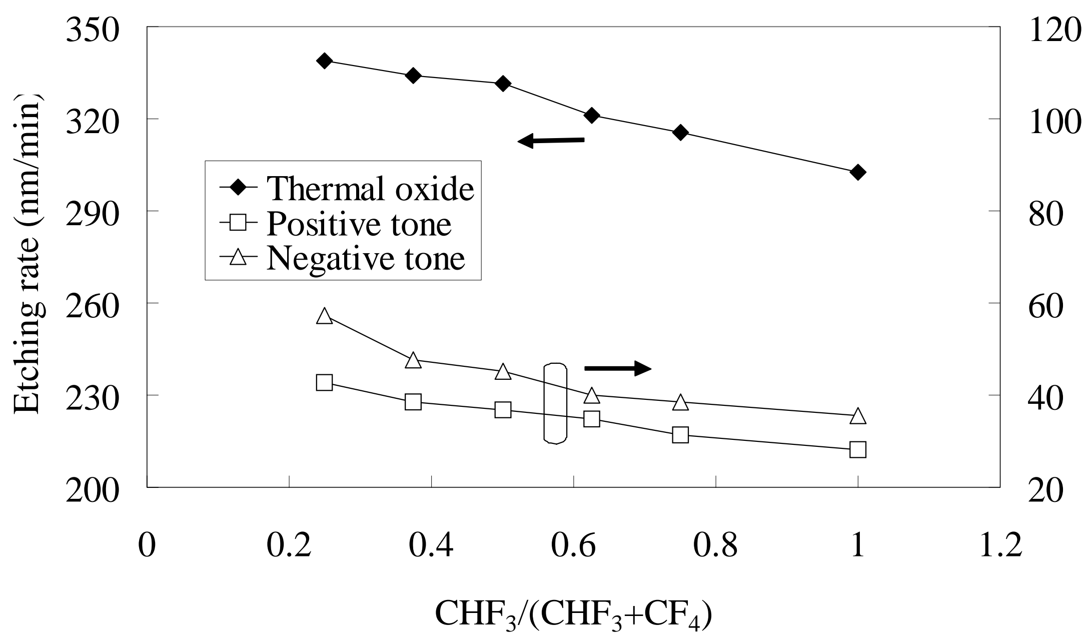

(b)

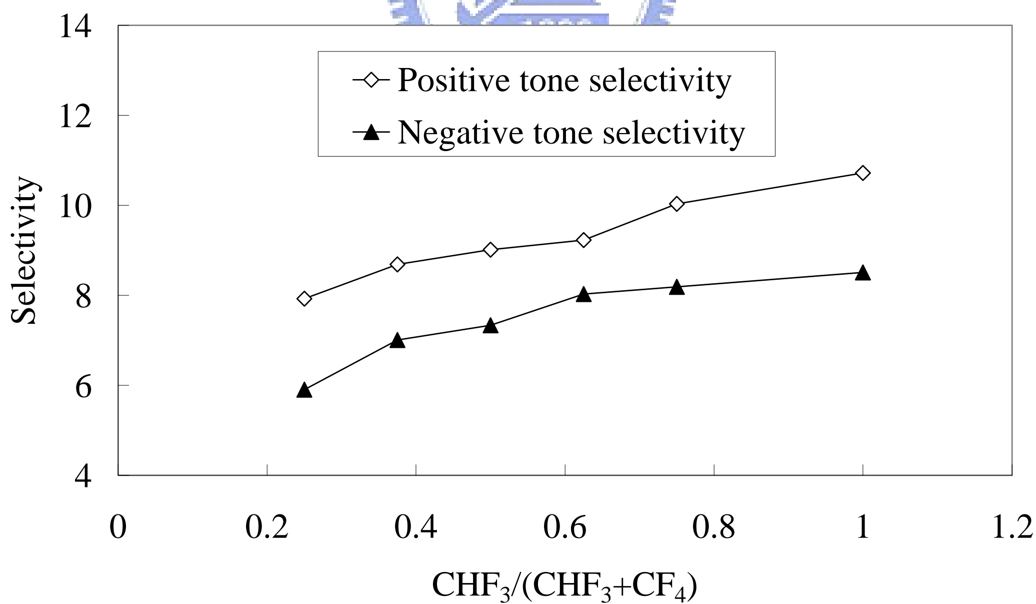

Figure 4-9. (a) Etching rate and (b) etching selectivity of the zwitter-polymer resist.